

FATIGUE CHARACTERIZATION OF A VAWT BLADE MATERIAL*

J. A. Van Den Avyle, Mechanical Metallurgy Division
H. J. Sutherland, Wind Energy Research Division
Sandia National Laboratories
Albuquerque, New Mexico

ABSTRACT

The fatigue analysis of Wind Energy Conversion System blades has been limited by the lack of fatigue data for typical blade materials, including 6063 aluminum, an alloy commonly used for Vertical Axis Wind Turbine (VAWT) blades. This paper reports results to date of a testing program to establish a fatigue properties database for this alloy. Two types of fatigue response data were measured: 1) stress versus number of cycles to failure (S-n) and 2) fatigue crack growth rates. S-n experiments have been conducted on 6063 aluminum blade extrusion material using approximately 100 bend specimens cycled at five alternating stress amplitudes and at four mean stress levels. Data have been analyzed using an equivalent alternating stress based on Goodman's rule to describe mean stress effects on fatigue life. Cyclic crack growth rates have been measured using three loading ratios.

NOMENCLATURE

a _b	-	constants in linear regression fit to Goodman analysis
A _m	-	constants in crack growth rate equation
da/dn	-	cyclic crack propagation rate, mm/cycle
K _{max}	-	maximum applied stress intensity factor in fatigue loading cycle, MPa ^{1/2}
K _{min}	-	minimum applied stress intensity factor in fatigue loading cycle, MPa ^{1/2}
ΔK	-	K _{max} -K _{min} , MPa ^{1/2}
n	-	number of loading cycles in fatigue
n _f	-	number of cycles to failure
R	-	loading ratio, K _{min} /K _{max}
r ²	-	linear least squares correlation coefficient
S _{al}	-	alternating stress in fatigue cycle, MPa
S _e	-	effective alternating stress, MPa
S _m	-	mean stress in fatigue cycle, MPa
S _u	-	ultimate tensile strength, MPa
S _y	-	yield strength, MPa

INTRODUCTION

One form of Vertical Axis Wind Turbine (VAWT) blades uses large, hollow, internally ribbed extrusions made of aluminum alloy 6063-T5; such extrusions are typically produced up to 16 m long with a wall thickness of 6.4 mm. This alloy was selected primarily because of its ease of extrusion into large shapes. Its mechanical strength properties are moderate (1) and have not typically been important criteria for previous industrial applications, such as architectural trim. For this reason few earlier data have been generated to characterize the fatigue behavior of 6063 aluminum; the only published source found reports rotating bending-generated stress versus cycles to failure (S-n) data (2).

This paper reports results to date of an experimental testing program to establish a fatigue properties database for this alloy. Existing design methods can require either of two types of fatigue response data: 1) stress versus number of cycles to failure (S-n) and 2) fatigue crack growth rates. S-n testing measures total cyclic life as a function of applied alternating stress amplitude and mean stress level; multiple tests at a given condition are generally run to provide statistical significance.

Sandia National Laboratories has sponsored a series of beam bending fatigue tests to determine the S-n characteristics of extruded 6063-T5 aluminum. The majority of the testing has been performed under contract at Teledyne Engineering Services (3); the test matrix includes 5 alternating stress levels at each of 4 mean stress levels being cycled to a maximum of 5X10⁸ cycles. In addition, Southern University (4) has conducted beam bending fatigue experiments on the same extrusion material (sponsored by the Solar Energy Research Institute, Boulder, CO). This work has utilized the same specimens and testing setup as

*This work performed at Sandia National Laboratories supported by the U. S. Department of Energy under contract number DE-AC04-76DP00789.

the Teledyne work, so the data is compatible; a total of 20 experiments have been run at Southern to date.

Fatigue crack growth rate tests have been performed on extrusion material to measure the cyclic propagation rate (da/dn) as a function of applied cyclic stress intensity (ΔK) for different values of loading ratio R , where $R=K_{min}/K_{max}$. These data are required for a fracture mechanics-based design procedure where structural fatigue life is determined by a flaw growth criterion.

Aluminum alloy 6063 is an age hardenable alloy of nominal composition 0.4% Si, 0.7% Mg, with balance Al (all in weight percent) (1). Typical commercial strength levels for differing aging treatments are listed in Table 1. The extrusion material tested here was purchased to a -T5 aged minimum strength level specification. This condition is produced by rapidly air-quench cooling from the extrusion press followed by an aging treatment of 175°C for 6 h.

EXPERIMENTAL

Tensile test and fatigue specimens were sectioned from the outer skin (6.4 mm thick) of a VAWT blade extrusion that was manufactured by Spectrulite Consortium, Inc., Madison, IL. Their stress axes were parallel to the blade length so that cracking was in the transverse direction across the blade chord. Tensile specimens were rectangular in cross-section with gage dimensions 50 mm long X 13 mm wide X 5.1 mm thick. These were run at room temperature at a strain rate of $5 \times 10^{-3} \text{ s}^{-1}$.

The S-n specimen was a tapered constant-stress cantilever bending design (Fig. 1). Sample machining and surface preparation were specified to minimize surface and sub-surface damage which could potentially affect initiation of fatigue cracks and to provide specimen to specimen uniformity. Final surface finishing was done using 600 grit SiC paper. Tests were performed using a Fatigue Dynamics, Inc. reversed bending fatigue test machine at cyclic rates up to 87 cy/s. An instrumented specimen grip was designed to dynamically monitor loads during cycling to minimize test setup variations on fatigue life.

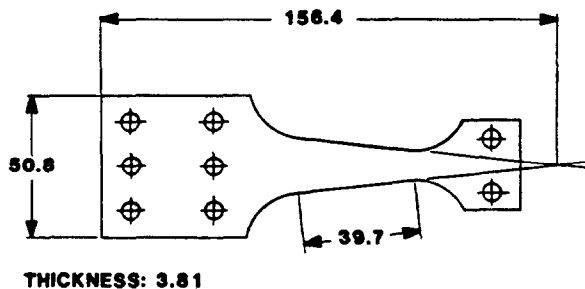


Fig. 1 Schematic S-n specimen design using tapered constant stress cantilever bending geometry; dimensions in mm.

Fatigue crack growth rate testing was conducted in accordance with ASTM specification E 647-86 using an MTS servohydraulic test frame at a frequency

of 20 cy/s. The specimen was a standard compact tension design with a thickness of 3.8 mm and a width of 76.2 mm. Tests were cycled at constant load ranges, and crack lengths were monitored optically at 20X magnification. From measured pairs of crack length and cycle number taken at 0.5 mm intervals, crack growth rates were calculated using the 7-point incremental polynomial method outlined in the specification.

Several tensile and fatigue crack growth test specimens were heat treated to the commercial -T6 peak aged condition to compare properties with the -T5 extrusion. Starting from the extrusion material, these specimens were solutionized in air at 525°C, quenched in water, and subsequently aged at 175°C for 6 h.

RESULTS AND DISCUSSION

Measured tensile properties of the -T5 extrusion and peak aged -T6 conditions are listed in Table 1 along with nominal handbook values (1). Strengths of measured -T5 and -T6 are similar, with somewhat lower yield and higher ultimate strengths for the -T5 extrusion. Both these values are similar to the handbook level for -T6, which is much higher than the nominal -T5. These strength properties

Table 1. Tensile Properties of 6063 Aluminum

	s_y (MPa)	s_u (MPa)	% Elong
<u>Nominal (1)</u>			
-T4	90	170	22
-T5	145	185	12
-T6	215	240	12
<u>Measured</u>			
-T5	205	245	---
-T6	217	236	---

indicate that the rate of cooling from the extrusion temperature, estimated to be 3.5°C s^{-1} from 560°C, is rapid enough to maintain the alloying elements in solution during cooldown and allow a precipitation reaction to occur during subsequent aging. Extensive microstructural examinations of these and other heat treatments for this alloy are reported elsewhere (5).

S-n Data

Results of the S-n tests completed to date by the two laboratories out to lifetimes of 1×10^8 cycles are shown in Fig. 2. The data are arranged into four tensile mean stress values between 0 and 103.5 MPa, and linear least squares curve fits through each mean stress data set are given to help show the trends in behavior. As expected, higher mean stresses promote shorter fatigue lives. At the highest cycles to failure the scatter increases somewhat and there is an indication that the slope of the data curves may decrease.

The S-n data has been fit with a number of proposed constitutive formulations (6). These included a Goodman fit using the yield strength of the material (s_y), a Goodman fit using the ultimate strength of the material (s_u), a Gerber fit, and a

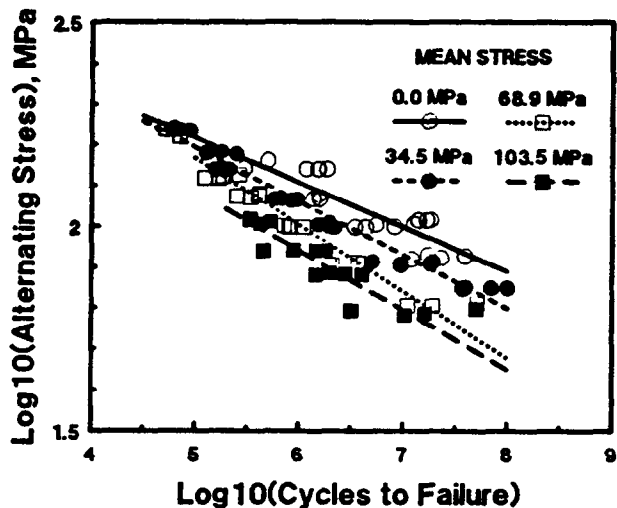


Fig. 2 Results of S-n testing of 6063-T5 aluminum

modified Gerber fit. For these fits, the standard deviations between the data and the fits were found to be 0.1332, 0.04290, 0.04752 and 0.03632, respectively (the modified Gerber fit optimized with the exponent equal to 1.28). From these calculations, Goodman's rule using s_u and the modified Gerber fit both yield small standard deviations, but Goodman's rule is simpler to apply, and it has one less adjustable parameter.

As used here, the Goodman rule states that the fatigue life at an alternating stress s_{al} and a mean stress s_m is equivalent to the fatigue life at an equivalent alternating stress s_e at zero mean stress by:

$$s_{al} = s_e (1 - s_m / s_u) . \quad (1)$$

From the tensile tests, $s_u = 245$ MPa (35.4 ksi). The fatigue data gathered by Teledyne and Southern University are plotted in Fig. 3 using this formulation. Also shown in this figure is a least-squares curve fit to the data. The form chosen here is:

$$\log_{10}(s_e) = a + b \log_{10}(n_f) . \quad (2)$$

where n_f is the number of cycles to failure. The data fit yields values of 2.93421 for a and -0.13256 for b , with a standard deviation of 0.04290 (units of stress are MPa). This curve fit is the solid line shown passing through the center of the data in Fig. 3. The dashed lines in the figure are the curves for two standard deviations above and below the norm (i.e., $a = 2.93421 \pm 2 [0.04290]$ and $b = -0.13256$ in Eq. 2).

This curve fit is not the optimum fit of the data. If s_u is taken to be 317 MPa (46 ksi), the standard deviation can be reduced from 0.04290 to 0.03552. However, the 317 MPa is not a realistic value for s_u .

These data may be compared to fatigue data from rotational bending tests. In Fig. 4, the data are plotted with design data reported in Ref. 2 for the -T5 and the -T6 conditions. As seen in this figure, the flexural data reported here lie slightly above the -T6 design curve at relatively low cycles to failure. This is reasonable since the extrusion material is similar in

strength to nominal -T6 levels. At the high cycles to failure, the design data show a change in slope (at approximately 5×10^6 cycles to failure). As the data reported here do not extend past 1×10^8 cycles, a slope change may or may not be present. Remaining tests out to lifetimes of approximately 5×10^8 cycles may indicate whether there is a slope change.

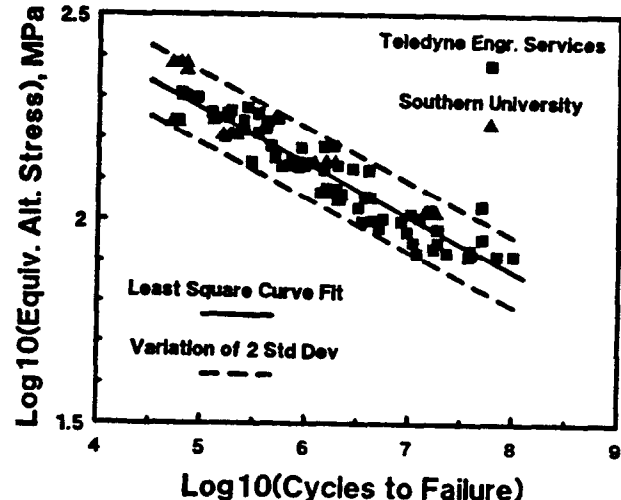


Fig. 3 S-n data of 6063-T5 aluminum plotted with Goodman fit using ultimate strength to calculate effective alternating stress

Crack Growth Rate Data

The fatigue crack growth behavior of 6063-T5 aluminum is shown in Fig. 5, plotting growth rate (da/dn) versus applied stress intensity factor range (ΔK) at loading ratio, R , levels of 0.09, 0.3, and 0.5. The curves at $R = 0.09$ and 0.5 are combined data from at least three separate tests, while the curve at $R = 0.3$ is a single test. The data are linear on this log-log scale, which indicates a power law dependence of the form:

$$da/dn = A \Delta K^{(m)} \quad (3)$$

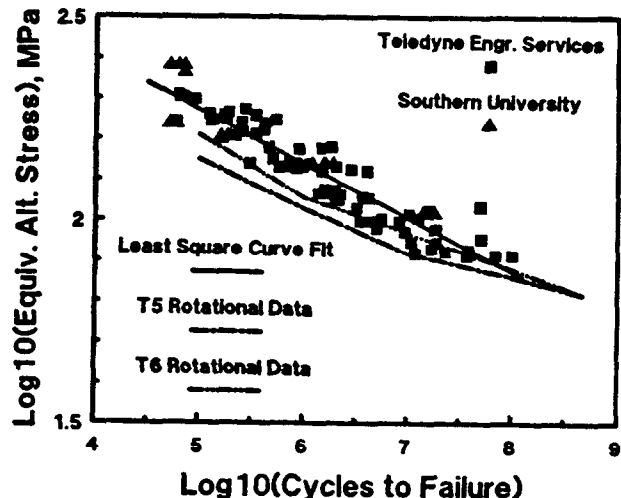


Fig. 4 Measured S-n data compared to design data for 6063-T5 and -T6 aluminum from Ref. 2

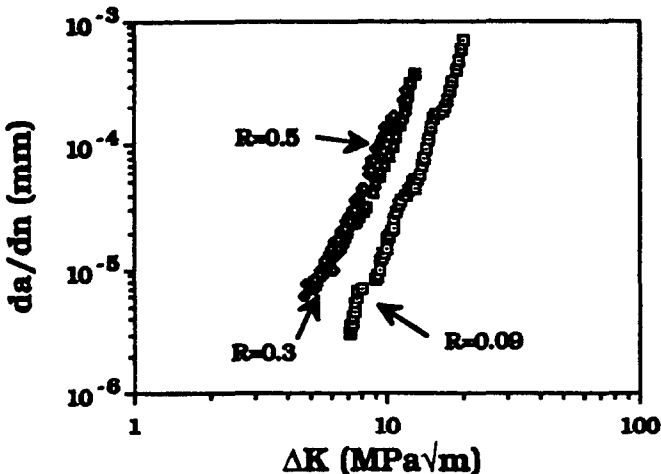


Fig. 5 Fatigue crack growth response of 6063-T5 aluminum

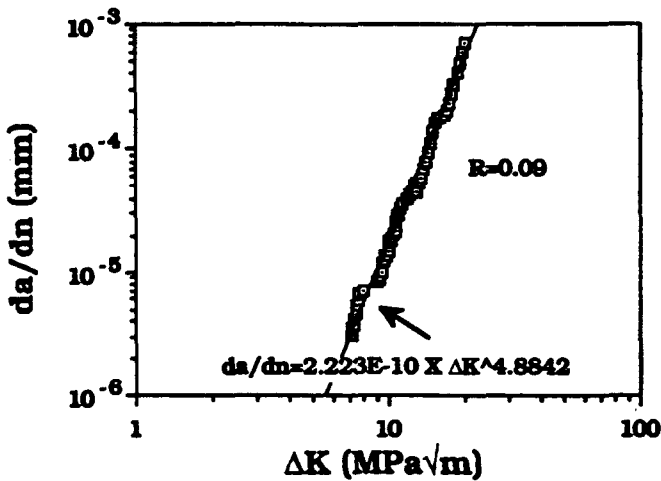


Fig. 6 Crack growth of 6063-T5 aluminum at $R=0.09$ with least-squares curve fit to data

A least-squares curve fit through the data for $R = 0.09$ is shown in Fig. 6; this is typical of the other fits. Values of the constants A and m in Eq. 3 for each R ratio are:

R	A	m	R^2
0.09	2.223×10^{-10}	4.8842	0.99
0.30	1.037×10^{-8}	3.9224	0.98
0.50	1.100×10^{-8}	4.0099	0.98

This power law dependence with $m=4$ is consistent with other data for aluminum and other alloys in the growth rate range 10^{-6} to 10^{-3} mm/cycle, which is above the fatigue crack growth threshold (7).

For a given ΔK the growth rates increase with increasing R ratio (Fig. 5). This R ratio effect is commonly observed and is attributed substantially to early crack closure (8). Crack closure occurs during the unloading portion of the fatigue cycle when separated crack surfaces touch before the applied load reaches its minimum level; during reloading, a finite

load, termed the opening load, must be reached before the crack separates fully and opening stress is applied to the crack tip. Thus only a portion of the full loading cycle or applied ΔK is used to strain the crack tip to cause crack growth. At higher R ratios with higher tensile mean stress, a larger fraction of the applied ΔK acts to strain the crack tip, and growth rates are faster.

Rough crack surfaces tend to promote early closure because of interference between surface asperities (8). Examinations of fatigue specimen fracture surfaces visually and in the scanning electron microscope (SEM) show a very rough morphology where the crack primarily follows grain boundaries (Fig. 7). The fracture surface is mostly intergranular with small interconnecting transgranular regions;



Fig. 7 Rough intergranular fatigue fracture surface of 6063-T5 aluminum (scanning electron micrograph)

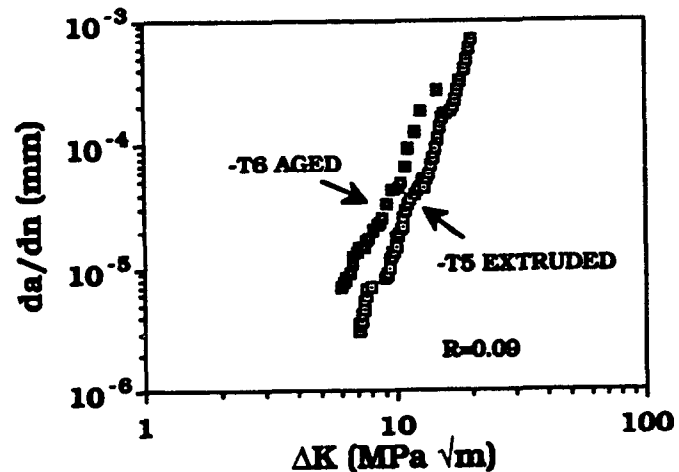


Fig. 8 Lower fatigue crack growth rates for 6063-T5 aluminum compared to -T6 at $R=0.09$

this mode is also seen in tensile overload fractures in the -T5 extruded and aged alloy. The grain size is large at approximately 200 μm , which contributes to the rough surfaces. The thermal treatment these extrusions experience produces a microstructure with large grain size and other grain boundary features which cause intergranular fracture (5).



Fig. 9 Smoother transgranular fatigue fracture surface of 6063-T6 aluminum (scanning electron micrograph)

To further study this effect, samples were heat treated to the -T6 aged condition, which has the same strength level and grain size as the as-received -T5 material (Table 1). Crack growth rates at $R = 0.09$ are higher for the -T6 specimen (Fig. 8). The fatigue fracture changed to a transgranular mode which features a much flatter surface (Fig. 9). Due to the smoother surfaces, the crack closure effect is less, and growth rates are higher.

Fatigue crack growth rates of the 6063-T5 extrusions are beneficially lowered due to microstructural features produced by the thermal history of the extrusion process. It is uncertain what effect this microstructure has on the process of crack initiation. Current research is investigating the mechanisms of crack initiation in this alloy (9).

CONCLUSIONS

1. Results of S-n fatigue testing of 6063-T5 aluminum alloy at five alternating stress levels and four mean stress levels can be correlated by a Goodman fit using the ultimate strength to calculate an equivalent alternating stress.
2. Fatigue crack growth rates follow a power law relationship with ΔK over the range of growth rates studied. Crack growth has been measured at three loading ratios (R).

3. Reduced growth rates are measured in 6063-T5 extrusions compared to 6063-T6 laboratory-aged to the same strength level. This is attributed to crack closure effects caused by rough intergranular fracture surfaces in 6063-T5.

ACKNOWLEDGEMENTS

The authors wish to acknowledge the contributions of Paul Hatch of the Mechanical Metallurgy Division at Sandia National Laboratories who performed fatigue crack growth measurements and Dave Johnson and Richard Greeno of Teledyne Engineering Services and Habib Mohamadian and Ira Graham of Southern University who performed S-n fatigue testing.

REFERENCES

1. Hatch, J. E., ed., 1984, Aluminum: Properties and Physical Metallurgy, American Society for Metals, Metals Park, OH, pp 362-368.
2. Military Handbook, 1966, MIL-HDBK-694A(MR), p 51.
3. Teledyne Engineering Services, 130 Second Avenue, Waltham, MA 02254
4. Mohamadian, H. P. and Graham, I. J., Southern University, Baton Rouge, LA, personal communication, July 1988.
5. Van Den Avyle, J. A. and Hills, C. R., "Effects of Precipitate Free Zones on Fatigue Crack Propagation in 6063-T5 Aluminum Extrusions", to be published.
6. Osgood, C. C., 1962, Fatigue Design, 2nd Edition, Pergamon Press, Oxford, UK.
7. Paris, P. C., 1964, Fatigue--An Interdisciplinary Approach, Proceedings 10th Sagamore Conference, Syracuse University Press, Syracuse, NY, p107.
8. McEvily, A. J., 1988, "On Crack Closure in Fatigue Crack Growth", Mechanics of Fatigue Crack Closure, ASTM STP 982, American Society for Testing and Materials, Philadelphia, pp 35-43.
9. Pelloux, R. M. and Warren, A. S., Dept. of Materials Science and Engineering, Massachusetts Institute of Technology, Cambridge, MA, personal communication, 1988.

